

Marginal blind deconvolution of adaptive optics retinal images

L. Blanco^{1,2,3,*} and L. M. Mugnier^{1,3}

¹ONERA - The French Aerospace Lab, F-92322 Châtillon, France

²LESIA-Observatoire de Paris, CNRS, UPMC Univ Paris 06, Univ. Paris-Diderot, France

³Groupement d'Intérêt Scientifique PHASE (Partenariat Haute résolution Angulaire Sol Espace) between ONERA, Observatoire de Paris, CNRS and Université Paris Diderot, France

*leonardo.blanco@onera.fr

Abstract: Adaptive Optics corrected flood imaging of the retina has been in use for more than a decade and is now a well-developed technique. Nevertheless, raw AO flood images are usually of poor contrast because of the three-dimensional nature of the imaging, meaning that the image contains information coming from both the in-focus plane and the out-of-focus planes of the object, which also leads to a loss in resolution. Interpretation of such images is therefore difficult without an appropriate post-processing, which typically includes image deconvolution. The deconvolution of retina images is difficult because the point spread function (PSF) is not well known, a problem known as blind deconvolution. We present an image model for dealing with the problem of imaging a 3D object with a 2D conventional imager in which the recorded 2D image is a convolution of an invariant 2D object with a linear combination of 2D PSFs. The blind deconvolution problem boils down to estimating the coefficients of the PSF linear combination. We show that the conventional method of joint estimation fails even for a small number of coefficients. We derive a marginal estimation of the unknown parameters (PSF coefficients, object Power Spectral Density and noise level) followed by a MAP estimation of the object. We show that the marginal estimation has good statistical convergence properties and we present results on simulated and experimental data.

© 2011 Optical Society of America

OCIS codes: (100.1455) Blind deconvolution; (170.4470) Ophthalmology; (010.1080) Adaptive optics; (100.3190) Inverse problems; (100.6890) Three-dimensional image processing.

References and links

1. J. Liang, D. R. Williams, and D. T. Miller, "Supernormal vision and high-resolution retinal imaging through adaptive optics," *J. Opt. Soc. Am. A* **14**, 2884–2892 (1997).
2. M. Glanc, E. Gendron, F. Lacombe, D. Lafaille, J.-F. Le Gargasson, and P. Léna, "Towards wide-field retinal imaging with adaptive optics," *Opt. Commun.* **230**, 225–238 (2004).
3. J. Rha, R. S. Jonnal, K. E. Thorn, J. Qu, Y. Zhang, and D. T. Miller, "Adaptive optics flood-illumination camera for high speed retinal imaging," *Opt. Express* **14**, 4552–4569 (2006).
4. A. Roorda, F. Romero-Borja, I. William Donnelly, H. Queener, T. Hebert, and M. Campbell, "Adaptive optics scanning laser ophthalmoscopy," *Opt. Express* **10**, 405–412 (2002).
5. L. Blanc-Féraud, L. Mugnier, and A. Jalobeanu, "Blind image deconvolution," in "Inverse Problems in Vision and 3D Tomography," A. Mohammad-Djafari, ed. (ISTE / John Wiley, London, 2010), chap. 3, pp. 97–121.
6. G. R. Ayers and J. C. Dainty, "Iterative blind deconvolution and its applications," *Opt. Lett.* **13**, 547–549 (1988).
7. L. M. Mugnier, T. Fusco, and J.-M. Conan, "Mistral: a myopic edge-preserving image restoration method, with application to astronomical adaptive-optics-corrected long-exposure images," *J. Opt. Soc. Am. A* **21**, 1841–1854 (2004).

8. R. J. A. Little and D. B. Rubin, "On jointly estimating parameters and missing data by maximizing the complete-data likelihood," *The American Statistician* **37**, 218–220 (1983).
9. J. C. Christou, A. Roorda, and D. R. Williams, "Deconvolution of adaptive optics retinal images," *J. Opt. Soc. Am. A* **21**, 1393–1401 (2004).
10. G. Hari Kumar and Y. Bresler, "Perfect blind restoration of images blurred by multiple filters: theory and efficient algorithms," *IEEE Trans. Image Processing* **8**, 202–219 (1999).
11. J. Idier, L. Mugnier, and A. Blanc, "Statistical behavior of joint least square estimation in the phase diversity context," *IEEE Trans. Image Processing* **14**, 2107–2116 (2005).
12. E. Lehmann, *Theory of point estimation* (John Wiley, New York, NY, 1983).
13. A. Blanc, L. M. Mugnier, and J. Idier, "Marginal estimation of aberrations and image restoration by use of phase diversity," *J. Opt. Soc. Am. A* **20**, 1035–1045 (2003).
14. Y. Goussard, G. Demoment, and J. Idier, "A new algorithm for iterative deconvolution of sparse spike," in "ICASSP," (1990), pp. 1547–1550.
15. J.-M. Conan, L. M. Mugnier, T. Fusco, V. Michau, and G. Rousset, "Myopic deconvolution of adaptive optics images by use of object and point-spread function power spectra," *Appl. Opt.* **37**, 4614–4622 (1998).
16. É. Thiébaud, "Optimization issues in blind deconvolution algorithms," in "Astronomical Data Analysis II," vol. 4847, J.-L. Starck and F. D. Murtagh, eds. (Proc. Soc. Photo-Opt. Instrum. Eng., 2002), vol. 4847, pp. 174–183.

1. Introduction

Early detection of retinal pathologies such as glaucoma, age related macula degeneration (AMD) or retinitis pigmentosa (RP) is crucial in dealing with these conditions and calls for in vivo eye fundus imaging with a cellular level resolution, typically to be able to visualize and count the retina photoreceptors. Adaptive optics (AO) flood illumination retinal imaging allows for such a high resolution imaging and has now been used for more than a decade [1, 2, 3].

However, AO flood imaging suffers from an intrinsic limitation that decreases image quality and makes both automatic post-processing (photoreceptor counting, blood vessel diameter measurements...) and visual interpretation difficult: the three-dimensional nature of the object and of the imaging process. Indeed, information from both the in-focus plane and out-of-focus planes in front of and behind the in-focus plane contribute to the final 2D image, which creates an important background that reduces image contrast and leads to a loss in resolution.

A hardware solution to this problem is Adaptive Optics Scanning Laser Ophthalmoscopy [4] (AO-SLO): by using a confocal pinhole, one selects only the photons coming from a specific layer of the tissue under examination.

An alternative software solution for mitigating these effects without any setup modification is image deconvolution. Retinal image deconvolution is difficult for two reasons:

- imaging is fundamentally 3D and we only record 2D images. This aspect should be taken into account in the image model in order to enable a high-quality deconvolution ;
- the point spread function (PSF) is not well known, therefore we must estimate the PSF together with the object, a technique known as blind deconvolution.

In this paper, we focus on the imaging of the photoreceptor layer of the retina. In order to deal with the lack of information associated with recording only 2D images of a 3D object, we propose an imaging model in which the photoreceptor layer is assumed to be approximately shift invariant along the optical axis of the imaging system (*i.e.*, the photoreceptor size does not vary significantly over the depth of focus of the instrument and the photoreceptor are more or less parallel to the optical axis). We show that this hypothesis, although it is a simplifying one, is very effective on experimental AO retinal images with a visible and measurable effect on the lateral resolution of the images. Section 2 presents the imaging model and the PSF parameterization we will use. In Section 3, we describe the joint estimation of the object and the PSF before showing, both on simulation and theoretically, that it is not suited for our problem.

In Section 4, we derive a marginal estimator and show its performance on simulation. In Section 5, we show results of blind marginal deconvolution of experimental in vivo retinal images. Section 6 summarizes the results.

2. Imaging model and PSF parameterization

The object and the imaging process are both three-dimensional (3D). If we record a stack i_{3D} of 2D images focused at different depths in the object, a reasonable image formation model, after background subtraction, can be written as a 3D convolution:

$$\mathbf{i}_{3D} = \mathbf{h}_{3D} *_{3D} \mathbf{o}_{3D} + \mathbf{n}, \quad (1)$$

where \mathbf{i}_{3D} is the 3D image, \mathbf{o}_{3D} is the 3D object, $*_{3D}$ denotes the 3D convolution operator, \mathbf{h}_{3D} is the 3D PSF and \mathbf{n} is the noise.

We assume that our object is shift invariant along the optical axis:

$$o_{3D}(x, y, z) = o_{2D}(x, y) \alpha(z), \quad (2)$$

where $\alpha(z)$ is the normalized flux emitted by the plane at depth z ($\int \alpha(z) dz = 1$).

Strictly speaking, this assumption means that our object must be shift invariant in z over an infinite range. However, in practice this invariance must only be verified over the depth of focus of the instrument ($\approx 50 \mu m$ for an AO flood imager, $\approx 10 - 15 \mu m$ for a confocal imager). Indeed, planes farther than the depth of focus from the image plane contribute to the image with a PSF that has a very narrow spectrum thus their contribution is almost a constant background.

In our case, we assume that the lateral size of the photoreceptors does not vary significantly and that the photoreceptors are almost parallel to the optical axis. Additionally, the depth of focus is about the length of a cone photoreceptor. Hence, the structures in front and behind the photoreceptor layer (pigment epithelium or inner retina layers) are way out of focus and only contribute as a background.

Current flood imaging systems only record data in one plane of interest. Using Eq. (1) and Eq. (2), it is easy to show that, in plane $z = 0$ for instance:

$$\begin{aligned} i(x, y) &\triangleq i_{3D}(x, y, z)|_{z=0} \\ &= \iiint \alpha(-z') h_{3D}(x', y', z') o_{2D}(x - x', y - y') dx' dy' dz' + n(x, y) \\ &= (h_{2D} o_{2D} *_{2D})(x, y) + n(x, y), \end{aligned} \quad (3)$$

with h_{2D} an *effective* 2D PSF which depends on the longitudinal brightness distribution of the object $\alpha(z)$ and on the 3D PSF:

$$h_{2D}(x, y) = \int \alpha(-z) h_{3D}(x, y, z) dz.$$

The 2D image $i(x, y)$ at the focal plane of the instrument is the 2D convolution of a 2D object and a global PSF h which is the linear combination of the individual 2D PSFs (each one conjugated with a different plane of the object) weighted by the back-scattered flux at each plane.

After discretization and using Riemann sum to approximate the integral:

$$h_{2D}(x, y) \approx \sum_j \alpha_j h_j(x, y), \quad (4)$$

with $h_j(x, y) \triangleq h_{3D}(x, y, z_j)$ the 2D lateral PSF at depth z_j and $\alpha_j = \alpha(z_j) \Delta z_j$ where Δz_j is the effective thickness of the j th layer. We define $\alpha = \{\alpha_j\}_j$ as the vector of unknowns that

parameterize the PSF. α is normalized ($\sum \alpha_j = 1$) and each parameter is positive ($\alpha_j \geq 0$). We search for h_{2D} as a linear combination of a basis of PSF's, each corresponding to a given plane. In the following, we consider short-exposure diffractive PSF's so that each h_j can be computed from the residual aberrations measured with a WFS and the knowledge of the defocus of plane z_j .

3. Joint estimation

There is a large body of work on blind deconvolution, originating in good part from astronomy (see, *e.g.*, Blanc-Féraud [5]). The conventional blind deconvolution approach is to perform an estimation of both the object and the PSF, jointly (see, *e.g.*, Ayers [6] for pioneering works and Mugnier [7] for more recent results on astronomical data).

3.1. Method

The joint estimation can be cast in a Bayesian framework as the computation of the joint maximum *a posteriori* (jmap) estimator:

$$(\hat{\mathbf{o}}, \hat{\alpha}) = \arg \max_{\mathbf{o}, \alpha} p(\mathbf{i}, \mathbf{o}, \alpha; \theta) \quad (5)$$

$$= \arg \max_{\mathbf{o}, \alpha} p(\mathbf{i}|\mathbf{o}, \alpha; \theta) \times p(\mathbf{o}; \theta) \times p(\alpha; \theta) \quad (6)$$

where, $p(\mathbf{i}, \mathbf{o}, \alpha; \theta)$ is the joint probability density of the data (\mathbf{i}), of the 2D object (\mathbf{o}), and of the PSF decomposition coefficients (α). It may depend on set of regularization parameters or hyperparameters (θ). $p(\mathbf{i}|\mathbf{o}, \alpha; \theta)$ is the likelihood of the data \mathbf{i} , $p(\mathbf{o}; \theta)$ is the *a priori* probability density function of the object \mathbf{o} and $p(\alpha; \theta)$ is the *a priori* probability density function of the coefficients α . In the following, we will not use any regularization on the set of coefficients α because we don't have any probability law for the PSF coefficients. However, since we only need to estimate a small number of these coefficients, this is not a problem.

The noise on the images is mainly photon noise which has a Poisson distribution. However, AO retinal images are dominated by a strong and quite homogeneous background. In the following, we will therefore assume that the noise is stationary white Gaussian with a variance σ^2 . For the object, we choose a stationary Gaussian prior probability distribution with a mean value \mathbf{o}_m and a covariance matrix \mathbf{R}_o . The set of hyperparameters is therefore $\theta = (\sigma^2, \mathbf{o}_m, \mathbf{R}_o)$. Under these assumptions, we have:

$$p(\mathbf{i}, \mathbf{o}, \alpha; \theta) = \frac{1}{(2\pi)^{\frac{N^2}{2}} \sigma^{N^2}} \exp \left(-\frac{1}{2\sigma^2} (\mathbf{i} - \mathbf{H}\mathbf{o})^t (\mathbf{i} - \mathbf{H}\mathbf{o}) \right) \\ \times \frac{1}{(2\pi)^{\frac{N^2}{2}} \det(\mathbf{R}_o)^{1/2}} \exp \left(-\frac{1}{2} (\mathbf{o} - \mathbf{o}_m)^t \mathbf{R}_o^{-1} (\mathbf{o} - \mathbf{o}_m) \right),$$

where \mathbf{H} is the operator performing the convolution by the PSF \mathbf{h} , $\det(x)$ is the determinant of matrix x and N^2 is the number of pixels in the image. $\hat{\mathbf{o}}$ and $\hat{\alpha}$ can therefore be defined as the estimated object and coefficients that minimize a criterion $J(\mathbf{o}, \alpha)$ defined as follows:

$$J_{\text{jmap}}(\mathbf{o}, \alpha) = J_i(\mathbf{o}, \alpha) + J_o(\mathbf{o}, \alpha), \quad (7)$$

where $J_i(\mathbf{o}, \alpha) = -\ln p(\mathbf{i}|\mathbf{o}, \alpha; \theta)$ (data-fidelity) and $J_o = -\ln p(\mathbf{o}; \theta)$ (regularization term). The criterion to be minimized reads:

$$J_{\text{jmap}}(\mathbf{o}, \alpha) = -\ln p(\mathbf{i}|\mathbf{o}, \alpha; \theta) - \ln p(\mathbf{o}; \theta) \quad (8)$$

$$\begin{aligned} J_{\text{jmap}}(\mathbf{o}, \alpha) &= \frac{1}{2}N^2 \ln \sigma^2 + \frac{1}{2\sigma^2}(\mathbf{i} - \mathbf{H}\mathbf{o})^t(\mathbf{i} - \mathbf{H}\mathbf{o}) \\ &+ \frac{1}{2} \ln \det(\mathbf{R}_o) + \frac{1}{2}(\mathbf{o} - \mathbf{o}_m)^t \mathbf{R}_o^{-1}(\mathbf{o} - \mathbf{o}_m) + C, \end{aligned} \quad (9)$$

where C is a constant. By cancelling the derivative of $J(\mathbf{o}, \alpha)$ with respect to the object, we obtain an analytical expression of the object $\hat{\mathbf{o}}(\alpha; \theta)$ that minimizes the criterion for a given $(\alpha; \theta)$:

$$\hat{\mathbf{o}}(\alpha, \theta) = (\mathbf{H}^t \mathbf{H} + \sigma^2 \mathbf{R}_o^{-1})^{-1}(\mathbf{H}^t \mathbf{i} + \sigma^2 \mathbf{R}_o^{-1} \mathbf{o}_m) \quad (10)$$

Since the matrices \mathbf{H} (convolution operator) and \mathbf{R}_o (covariance matrix of an object with a stationary probability density) are Toeplitz-block-Toeplitz, we can write the joint criterion J_{jmap} and the analytical expression of the object $\hat{\mathbf{o}}(\alpha, \theta)$ in the Fourier domain with a circulant approximation:

$$\begin{aligned} J_{\text{jmap}}(\mathbf{o}, \alpha) &= \frac{1}{2}N^2 \ln S_n + \frac{1}{2} \sum_{\mathbf{v}} \frac{|\tilde{i}(\mathbf{v}) - \tilde{h}(\mathbf{v})\tilde{o}(\mathbf{v})|^2}{S_n} \\ &+ \frac{1}{2} \sum_{\mathbf{v}} \ln S_o(\mathbf{v}) + \frac{1}{2} \sum_{\mathbf{v}} \frac{|\tilde{o}(\mathbf{v}) - \tilde{o}_m(\mathbf{v})|^2}{S_o(\mathbf{v})} \end{aligned} \quad (11)$$

$$\text{and } \hat{\mathbf{o}}(\alpha) = \frac{\tilde{h}^*(\mathbf{v})\tilde{i}(\mathbf{v}) + \frac{S_n}{S_o(\mathbf{v})}\tilde{o}_m(\mathbf{v})}{|\tilde{h}(\mathbf{v})|^2 + \frac{S_n}{S_o(\mathbf{v})}}, \quad (12)$$

where S_n is the noise power spectral density (PSD), S_o is the object PSD (the new set of hyperparameters in the Fourier domain is $\{S_n, S_o\}$), \mathbf{v} is the spatial frequency and \tilde{x} denotes the two-dimensional Fast Fourier Transform of x .

$\hat{\mathbf{o}}(\alpha)$ is the estimated object after classical Wiener filtering of the image \mathbf{i} and is easily computed.

If we substitute Eq. (12) into Eq. (11), we obtain a new expression of J_{jmap} that does not depend explicitly on the object:

$$\begin{aligned} J'_{\text{jmap}}(\alpha) &= \frac{1}{2}N^2 \ln S_n + \frac{1}{2} \sum_{\mathbf{v}} \ln S_o(\mathbf{v}) \\ &+ \frac{1}{2} \sum_{\mathbf{v}} \frac{1}{S_o(\mathbf{v})} \frac{|\tilde{i}(\mathbf{v}) - \tilde{h}(\mathbf{v})\tilde{o}_m(\mathbf{v})|^2}{|\tilde{h}(\mathbf{v})|^2 + \frac{S_n}{S_o(\mathbf{v})}}. \end{aligned} \quad (13)$$

The joint MAP solution is thus the pair $(\hat{\mathbf{o}}(\alpha), \alpha)$ for the value of α that minimizes Eq. 13.

3.2. Simulation results

The following simulation was performed to evaluate the performance of the joint estimator in our problem.

A simulated image is built in the following manner:

$$\mathbf{i} = (\alpha * \mathbf{h}_{\text{foc}} + (1 - \alpha)\mathbf{h}_{\text{defoc}}) * \mathbf{o} + \mathbf{n}, \quad (14)$$

where

- the global PSF is the sum of only two weighted PSF's, the first one \mathbf{h}_{foc} being focused and the second one $\mathbf{h}_{\text{defoc}}$ defocused. We assume that the focused PSF has no aberration (AO correction is perfect). The defocus is equal to π radian RMS;
- The object used is a 128×128 pixel portion of an experimental AO image obtained with the XV-XX retinal imager developed by the Observatoire de Paris [2];
- Noise \mathbf{n} is stationary Gaussian with a standard deviation $\sigma = 0.01 * \max(\mathbf{o})$, corresponding roughly to photon noise for an average of 10000 photons/pixel;
- $\alpha = 0.3$.

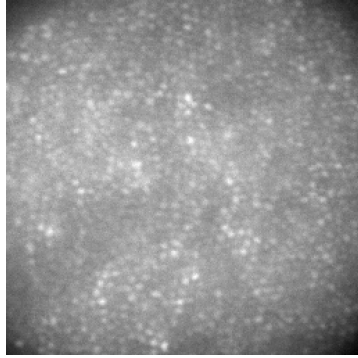


Fig. 1. Simulated object

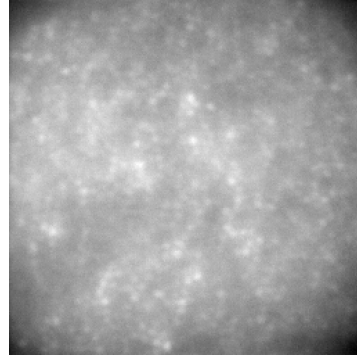


Fig. 2. Simulated image

We assume for the sake of this simulation that the object PSD S_o and the noise PSD S_n are known although it is not the case in practice. Therefore, we perform a so-called "supervised" estimation of α : we compute the joint criterion $J_{\text{jmap}}(\alpha; S_o, S_n)$ (see Eq. 13)) for values of α ranging from 0 to 1 to find the value of α that minimizes the joint criterion. Figure 3 shows the result of such a computation.

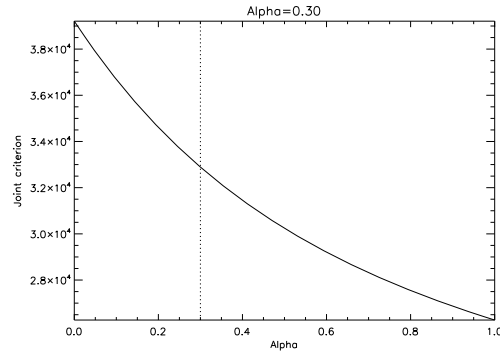


Fig. 3. Joint criterion for $0 \leq \alpha \leq 1$

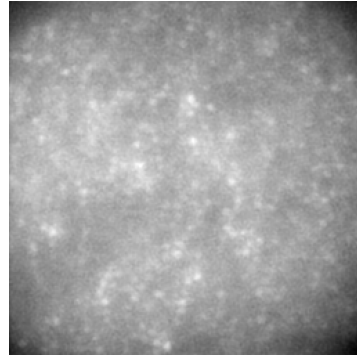


Fig. 4. Jointly estimated object

We see that the joint estimator is minimum for $\alpha = 1$ whereas the real value of α is 0.3. The joint estimation fails to retrieve the actual value even in this very simple case (two point spread functions, known hyperparameters). Figure 4 shows the restored object for the value of

α that minimizes $J_{\text{jmap}}(\alpha; S_o, S_n)$. The image is poorly deconvolved since the estimated PSF is perfectly focused whereas the actual global PSF is only 30% focused.

The joint estimator does not work well in the case of myopic deconvolution of retinal images, even in the most simple case of only two PSF's with known S_n and S_o . Actually, a close look at Eq. (13) helps us understand why this joint estimator is actually degenerate in this case: if, for instance, the mean object we use to compute the joint criterion is constant ($\mathbf{o}_m = \beta$), and since the PSF and the set of parameters are both normalized, then the numerator does not depend on the set of parameters α . Minimizing J'_{jmap} is equivalent to maximizing this denominator, *i.e.*, to choosing the PSF with the highest MTF $|\tilde{h}|$, which is the most focused PSF.

One might wonder why the joint estimation, although known to show poor results for blind deconvolution [8] is actually quite used in other contexts such as astronomical imaging. The joint estimation works fairly well thanks to constraints such as PSF support or positivity (which effectively acts as an object support constraint) that help remove ambiguities between the object and the PSF. In our case, since we cannot use such constraints (the photoreceptor signal is superimposed over a strong background and the object extends far beyond the recorded field of view of the system), the joint estimator is not well suited for retinal image deconvolution.

Multi-frame joint deconvolution [9] can help since it increases the number of data for the same object but is only effective if the PSFs are different enough [10], such as in the case of phase diversity [11]. Therefore, another estimator with better statistical properties would be preferable, ideally capable of restoring the PSF on a single frame.

4. Marginal estimation

The poor results of the joint estimation led us to propose another estimator for our imaging problem. The estimator proposed is the marginal estimator, which has better properties [12] and has never been used previously in retinal images deconvolution although it has already been proposed in the literature in other contexts including estimation of aberrations by use of phase diversity [13]. The principle of marginal estimation is to integrate the object \mathbf{o} out of the problem (*i.e.*, marginalize the posterior likelihood [5]). We integrate the joint probability of the object \mathbf{o} and the PSF parameters α over all the possible values of object \mathbf{o} .

$$\hat{\alpha} = \arg \max_{\alpha} \int p(\mathbf{i}, \mathbf{o}, \alpha; \theta) d\mathbf{o}. \quad (15)$$

Marginalization reduces the number of unknowns to be retrieved (from the total number of pixels of the image + the PSF parameters in the joint estimation case to just a few PSF parameters) and gives us a true maximum likelihood or maximum a posteriori (depending on the prior on the estimated parameters) estimator of the parameters of interest (namely, the PSF parameters). After estimation of the PSF parameters α , the object is restored by Wiener filtering of the image with the estimated global PSF and hyperparameters.

4.1. Marginal criterion

$$\hat{\alpha}_{\text{ML}} = \arg \max_{\alpha} p(\mathbf{i}, \alpha; \theta) = \arg \max_{\alpha} p(\mathbf{i} | \alpha; \theta) p(\alpha; \theta). \quad (16)$$

We keep the assumptions made for the joint estimation: a stationary white Gaussian noise with variance σ^2 , stationary Gaussian prior probability distribution with a mean value \mathbf{o}_m and covariance matrix \mathbf{R}_o for the object. Since \mathbf{i} is a linear combination of a Gaussian object and a Gaussian noise, it is also Gaussian. Its associated probability density reads:

$$p(\mathbf{i} | \alpha; \theta) = A(\det \mathbf{R}_i)^{-1/2} \exp \left(-\frac{1}{2} (\mathbf{i} - \mathbf{i}_m)' \mathbf{R}_i^{-1} (\mathbf{i} - \mathbf{i}_m) \right), \quad (17)$$

where A is a constant, \mathbf{R}_i is the image covariance matrix and $\mathbf{i}_m = \mathbf{H}\mathbf{o}_m$. Since we only need to estimate a small number of parameters, there is no need to regularize the solution over α . We therefore use a Maximum Likelihood (ML) estimator rather than a Maximum *A Posteriori* (MAP) estimator.

Maximizing $p(\mathbf{i}|\alpha; \theta)$ is equivalent to minimizing the opposite of its logarithm:

$$J_{\text{ML}}(\alpha) = \frac{1}{2} \ln \det(\mathbf{R}_i) + \frac{1}{2} (\mathbf{i} - \mathbf{i}_m)' \mathbf{R}_i^{-1} (\mathbf{i} - \mathbf{i}_m) + B \quad (18)$$

where B is a constant and $\mathbf{R}_i = \mathbf{H}\mathbf{R}_o\mathbf{H}' + \sigma^2 I_d$ (I_d is the identity matrix). The marginal criterion can be written in the Fourier domain as follows:

$$J_{\text{ML}}(\alpha) = \frac{1}{2} \sum_{\mathbf{v}} \ln S_o(\mathbf{v}) + \frac{1}{2} \sum_{\mathbf{v}} \ln \left(|\tilde{h}(\mathbf{v})|^2 + \frac{S_n}{S_o(\mathbf{v})} \right) + \frac{1}{2} \sum_{\mathbf{v}} \frac{1}{S_o(\mathbf{v})} \frac{|\tilde{i}(\mathbf{v}) - \tilde{h}(\mathbf{v})\tilde{o}_m(\mathbf{v})|^2}{|\tilde{h}(\mathbf{v})|^2 + \frac{S_n}{S_o(\mathbf{v})}} + B'. \quad (19)$$

Using Eq. 13 and Eq. 19, we obtain the following relationship between the marginal estimator and the joint estimator:

$$J_{\text{ML}}(\alpha) = J'_{\text{jmap}}(\alpha) + \frac{1}{2} \sum_{\mathbf{v}} \ln \left(|\tilde{h}(\mathbf{v})|^2 + \frac{S_n}{S_o(\mathbf{v})} \right) - \frac{1}{2} N^2 \ln S_n. \quad (20)$$

The marginal estimator is therefore very similar to the joint estimator in its mathematical expression (as shown by Goussard when the hyperparameters are known [14] and Blanc [13] for unknown hyperparameters. Its properties, as we will show in the following, are nevertheless significantly different to those of the joint estimator.

4.2. Marginal estimation results

We now present the results of the marginal estimation on simulated data. The same simulation as in the joint estimation was performed ($\mathbf{i} = (\alpha * \mathbf{h}_{\text{foc}} + (1 - \alpha)\mathbf{h}_{\text{defoc}}) * \mathbf{o} + \mathbf{n}$, with $\alpha = 0.3$). The marginal criterion of Eq. (19) was computed for $0 \leq \alpha \leq 1$ with known hyperparameters. The object is restored by Wiener filtering. Results of the computation are shown on figure 5 and the restored object on figure 6.

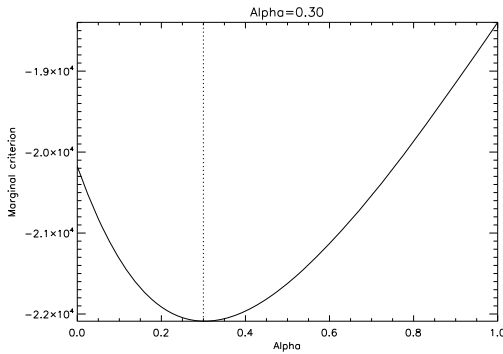


Fig. 5. Marginal criterion for $0 \leq \alpha \leq 1$

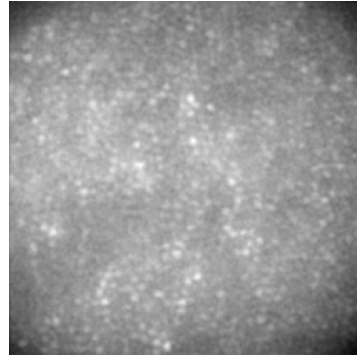


Fig. 6. Marginally estimated object

Figure 5 shows that marginal criterion is minimum for $\alpha = 0.3$, which is the true value of α used in the simulation. The marginal estimator accurately estimates the parameter of interest in our simulation. As a result, the restored object, shown in Figure 6, is much sharper than the simulated image and much closer to the actual object used in the simulation than the object restored with the joint estimation.

The marginal estimator thus enables supervised myopic deconvolution of retinal images with our image model. In practice, we do not have access to the true noise value and the true PSD of the object we are observing. Fortunately, the marginal estimator allows us to estimate these PSDs together with the PSF coefficients, as shown in the next paragraph.

4.3. Hyperparameter estimation

The marginal estimator allows us to estimate the set of hyperparameters θ (actually the object PSD S_o and noise PSD S_n) together with the PSF coefficients in an automatic manner. This method is called unsupervised estimation:

$$(\hat{\alpha}, \hat{S}_n, \hat{S}_o) = \arg \max_{\alpha, S_n, S_o} f(\mathbf{i}, \alpha; S_n, S_o). \quad (21)$$

In order to reduce the number of hyperparameters we must estimate, we choose to model the object PSD S_o in the following way [15]:

$$S_o(v) = \frac{k}{1 + \left(\frac{v}{v_0}\right)^p}. \quad (22)$$

Such PSD parametrization has been successfully used in various imaging applications such as astronomical imaging or earth observation from satellites. Since the noise is assumed to be Gaussian and homogeneous, $S_n = \text{constant}$. The criterion $J_{\text{ML}}(\alpha)$ becomes $J_{\text{ML}}(\alpha, S_n, k, v_0, p)$ and must now be minimized versus the PSF coefficients α and the hyperparameters S_n, k, v_0 and p .

With the change of variable $\mu = S_n/k$, if we cancel the derivative of the criterion with respect to k , we obtain an analytical expression for $\hat{k}(\alpha, \mu, v_0, p)$ that minimizes the criterion for a given value of the other parameters therefore only four hyperparameters remain, $\hat{\mu}$, \hat{v}_0 , \hat{p} and S_n [13].

PSF coefficients and hyperparameters are estimated in an alternate way. We initialize the algorithm with a perfectly focused global PSF.

There is no analytical expression for the minimum value of the criterion so the minimization has to be done numerically. In our case, the minimization is performed with a Variable Metric with Limited Memory, Bounded (VLM-B) method developed by E. Thiébaud [16].

4.4. Asymptotic properties

The maximum likelihood estimator is known to be a consistent estimator, *i.e.*, it tends toward the actual values of the estimated parameters as the noise tends toward zero or as the size of data tends toward infinity. It is also known to be asymptotically normal [12] so that the neg-log-likelihood is asymptotically quadratic thus convex.

Extensive simulations were performed to validate the statistical behavior of our unsupervised marginal estimation. The simulation conditions are the same as previously:

- $\mathbf{i} = (\alpha * \mathbf{h}_{\text{foc}} + (1 - \alpha)\mathbf{h}_{\text{defoc}}) * \mathbf{o} + \mathbf{n}$, with $\alpha = 0.3$;
- Noise RMS varies from 1% of the maximum value of the image to 20% of the maximum value of the image;

- 50 noise realizations were computed for each noise RMS value;
- The simulation was performed on 3 different subimages varying in size: a 32×32 pixel central region of image **i**, a 64×64 pixel central region of image **i** and the whole 128×128 pixel image **i**.

Figure 7 shows the RMS error on estimation of the PSF coefficients for the different values of noise and the varying data size, both in the supervised and unsupervised cases.

For a given data size and both in the supervised and unsupervised estimation, the marginal estimator RMS error tends towards zero (*i.e.*, the estimated parameters α tends towards the exact value) when noise decreases. Even more interestingly, for a given noise value, error tends towards zero as the size of data increases. In particular, for a 128×128 pixel image and for noise $\sigma = 5\%$ of the max value of the image, the RMS error on the PSF coefficient α estimation is less than 3%. For a noise RMS value of 1% of the image maximum, the unsupervised estimator basically shows the same performance as the supervised estimation.

This simulation shows that the unsupervised marginal estimator exhibits, in practice, its appealing theoretical properties, which opens the way to its use on experimental images.

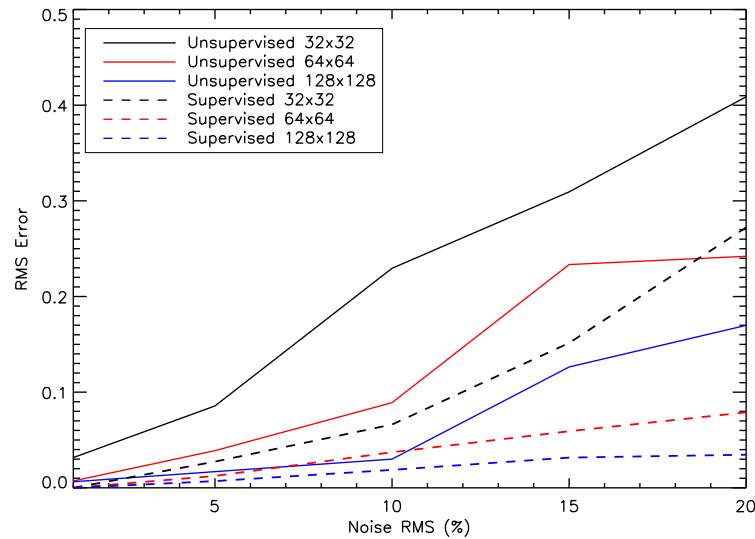


Fig. 7. RMS error on the estimation of the PSF coefficients as a function of noise level in percent (noise standard deviation over image maximum). The black, red and blue lines correspond, respectively, to 32×32 , 64×64 and 128×128 pixels images. Supervised case is in dashed lines, unsupervised case in solid line.

5. Preliminary experimental results

We now show experimental results of the marginal blind deconvolution on *in vivo* retinal images:

- The experimental image (Figure 8) is a 256×256 pixel image recorded on a healthy subject with the AO eye-fundus imager of the Center for Clinical Investigation of the Quinze-Vingts Hospital in Paris, developed by the Observatoire de Paris-Meudon [2];

- We model the global PSF as a linear combination of 3 PSFs, the first one being focused, the second one being defocused with a focus $\phi_1 = \pi/2$ rad RMS and the third one being defocused by $\phi_2 = \pi$ rad RMS.
- We assume that the adaptive optics has perfectly corrected the wavefront and that the focused PSF is a Airy disk.

We must estimate $\alpha = \{\alpha_1, \alpha_2, \alpha_3\}$.

The unsupervised marginal estimation gives $\alpha = \{0.24, 0.22, 0.54\}$, the resulting estimated PSF is shown on Figure 9. For this image, the main contribution (more than half of the energy) comes from the most out-of-focus plane and only a little less than 25% of the energy comes from the in-focus-plane.

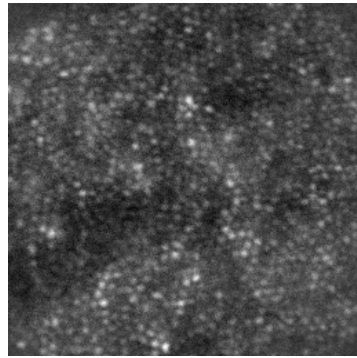


Fig. 8. Experimental image

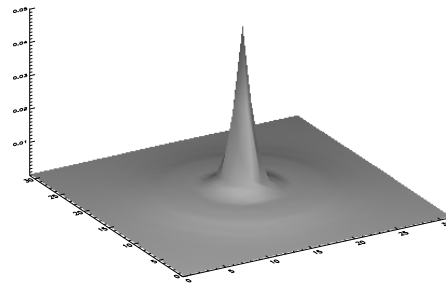


Fig. 9. Estimated PSF

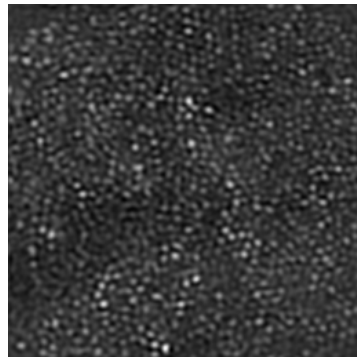


Fig. 10. Restored object

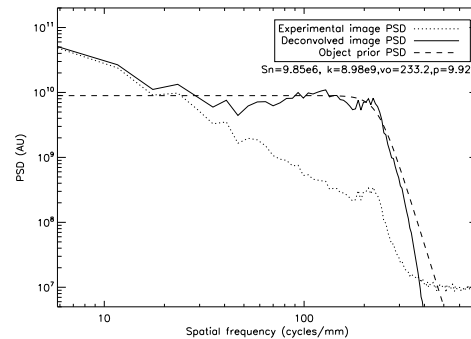


Fig. 11. PSD comparison between experimental image (dotted line), restored object (solid line) and object prior PSD (dashed line) with the estimated hyperparameters

The object is computed thanks to Eq. (12). Figure 10 shows the restored object after unsupervised marginal estimation. It is clearly visible that the restored object is much sharper than

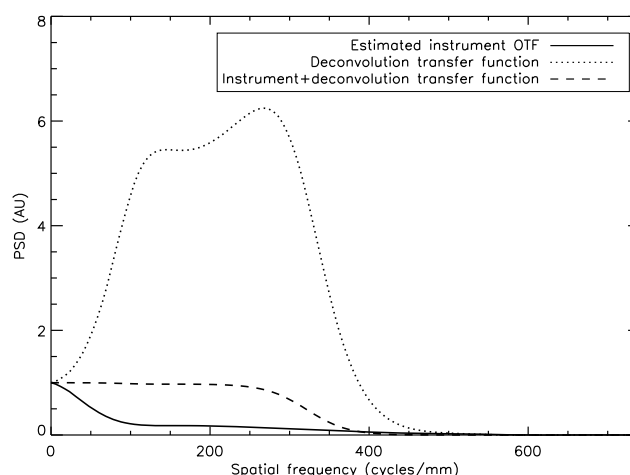


Fig. 12. Radial average of the estimated instrument optical transfer function, deconvolution transfer function and global (instrument+deconvolution) transfer function.

the original image. The photoreceptors have a much better contrast and can be seen clearly throughout the image. The restored object also is much less noisy than the original image.

Figure 11 shows a comparison of the power spectral densities of the experimental image and of the restored object: we can clearly see an improvement at the medium-high spatial frequency, with an improvement of a factor of 5 around 200-250 cycles/mm, *i.e.*, the spatial frequency corresponding to the cone photoreceptor size and separation. This frequency enhancement is clearly visible on Figure 12 that shows, in solid line, the estimated Optical Transfer Function (OTF) of our instrument (AO Flood imager+eye) as well as the deconvolution transfer function (dotted line) and the global (instrument+deconvolution) transfer function (dashed line). The deconvolution restores the spatial frequencies damped by the instrument transfer function up to 300 cycles/mm, a frequency that is beyond the spatial frequency of the cone photoreceptors in our image. These preliminary results show that our image model and the marginal estimator are well adapted to the deconvolution of adaptive optics corrected photoreceptor images. Motion artifacts due to eye movement during image acquisition and resulting in blurred images could possibly be addressed by changing the PSF basis to include motion induced PSFs and not only purely diffractive PSFs.

6. Conclusion

Blind deconvolution is a much needed tool for the interpretation and further processing of AO-corrected retinal images. We have proposed a reasonable imaging model to deal with the problem of only having 2D images of a 3D object that results in a useful PSF parameterization. We have shown, both analytically and through simulations, that the classical blind joint estimation of object and PSF is not suited for this problem. We have derived a marginal estimator of the PSF and extended it to estimate also the hyperparameters (object and noise PSDs), *i.e.*, to perform an unsupervised estimation. We have showed on simulations that this estimator is capable of restoring the PSF accurately even in the unsupervised case. The good statistical properties of the unsupervised marginal estimation have also been demonstrated.

Finally, we have shown preliminary results on experimental data, showing the efficiency

of the marginal estimator for myopic deconvolution of adaptive optics retinal images, with a measurable improvement of the contrast at the spatial frequencies corresponding to the cone photoreceptors. Although developed in the context of AO flood illumination retinal imaging, this marginal blind deconvolution method could also be applicable to other kinds of data such as confocal retinal imaging or more general microscopy data, or even astronomical data, mainly by changing the PSF basis used.

Acknowledgements

The authors are grateful to Marie Glanc for her support and her guidance on the use of the LESIA AO bench she designed and built.